Performance of Sheath Electric Field Measurement by Saturation Spectroscopy in Balmer-α Line of Atomic Hydrogen

Shusuke Nishiyama*, Kento Katayama, Haruhisa Nakano[1], Motoshi Goto[1], and Koichi Sasaki

Division of Quantum Science and Engineering, Hokkaido University, Sapporo 060-8628, Japan
[1]*National Institute for Fusion Science, Toki, Gifu 509-5292, Japan*

We developed a diode laser based system for measuring the sheath electric fields in low-temperature plasmas. The Stark spectrum of the Balmer-α line of atomic hydrogen was measured by saturation spectroscopy with a fine spectral resolution. The spectrum observed experimentally was consistent with the theoretical Stark spectrum, and we succeeded in evaluating the electric field strength on the basis of the experimental Stark spectrum. A sensitive detection limit of 10 V/cm was achieved by the developed system.

The electric fields in the sheath regions between plasmas and material surfaces play essential roles in various plasma processing technologies, since the sheath electric field accelerates positive ions toward the material surface.[1)] For example, the rate of plasma-aided dry etching is affected significantly by energetic positive ions that bombard the substrate surface.[2)] Hence, the understanding on the structure of the sheath electric field is of importance to optimize the plasma processing technologies. In addition, from the point of view of fundamental plasma physics, we still have insufficient knowledge on the structures of electric fields in a collisional sheath, a sheath with negative ions, a dynamic sheath driven by a pulsed voltage, *etc*.

The insufficient understanding on the sheath is caused by the difficulty in the measurement of the electric field. Since an emissive probe[3)] for measureing the electric potential has a limited spatial resolution and considerable disturbance to the plasma, a non-contact method with a fine spatial resolution is required. The non-contact method that has been investigated most intensively is laser Stark spectroscopy. The principle of laser Stark spectroscopy is measuring the energies of excited states which are perturbed by the electric field (the Stark effect). The Stark effect is more sensitive to an excited state with a higher potential energy. Hence various spectroscopic techniques to detect the energy of Rydberg states have been developed to date. Laser optogalvano spectroscopy[4–7)] and laser-induced collisional flu-

*E-mail address: shu@eng.hokudai.ac.jp

orescence spectroscopy[8–11] were used to detect the Rydberg states with principal quantum numbers of 8–10, resulting in the sensitivity of $\sim$ 200 V/cm for the electric field measurement. Much more sensitive measurements with sensitivities of 3-5 V/cm were demonstrated by laser-induced fluorescence-dip spectroscopy.[12–19] However, laser-induced fluorescence-dip spectroscopy requires two pulsed tunable lasers and sophisticated experimental skills. Therefore, an easy-to-use method with an economical cost is highly demanded in both the fields of plasma physics and plasma applications for measuring the sheath electric field.

The detection of Rydberg states is required because of the limited wavelength resolutions of the spectroscopic methods used in the conventional Stark spectroscopies. The wavelength resolutions in the Stark spectroscopies which has been developed to date are limited by the Doppler broadening of the transition line and the linewidth of the pulsed tunable laser. For example, the Doppler broadening width of the Balmer-α line of atomic hydrogen is approximately 10 GHz (15 pm) at a temperature of 1000 K. On the other hand, if we can use a spectroscopic method which has a much finer resolution, it is possible to detect the Stark effects of lower-laying energy states. An example is the work carried out by Adamov and coworkers.[20] They adopted two-photon absorption laser induced fluorescence (TALIF), which had a Doppler-free wavelength resolution, and detected the Stark effect of atomic hydrogen with a principal quantum number of $n = 3$. However, the TALIF measurement needs an expensive pulsed tunable laser at a wavelength of 205 nm.

In this work, we adopted saturation spectroscopy for detecting the Stark effect of the Balmer-α line of atomic hydrogen. Saturation spectroscopy has a Doppler-free wavelength resolution. In addition, a system of saturation spectroscopy at the Balmer-α line of atomic hydrogen can be constructed by employing a diode laser.[21] A diode laser is more economical than a pulsed tunable laser. In addition, the linewidth of a single-mode diode laser is much narrower than a pulse tunable laser. In this paper, we demonstrate the measurement of the Stark spectra of the Balmer-α line by saturation spectroscopy, and discuss the detection limit of the electric field.

Figure 1 shows the schematic of the experimental setup. A hydrogen plasma was generated in an inductively-coupled plasma source which was equipped with a one-turn internal rf antenna. One end of the antenna was connected to an rf power supply via a matching circuit, and the other end was connected to the vacuum chamber. The rf power was pulse modulated at a frequency of 20 kHz. The rf frequency, instantaneous power and the duty factor were 13.56 MHz, 1 kW and 50%, respectively. The vacuum chamber was a stainless-steel cylinder, and both the inner diameter and the height of the vacuum chamber were 26 cm. Pure

hydrogen was fed into the chamber via a mass-flow controller at a flow rate of 100 ccm. The gas pressure was 70 mTorr. A rectangular planer electrode with a size of 5×15 cm^2 was installed in the chamber. The electric potential of the electrode was grounded (the potential of the vacuum chamber). The distance between the electrode and the rf antenna was 5 cm. The electron density and the space potential of the plasma, which were measured using a Langmuir probe without placing the electrode, were approximately 1×10^{10} cm^{-3} and 8 V, respectively.

The light source for saturation spectroscopy was a linearly-polarized, single-mode diode laser (New Focus TLB-6900). The wavelength of the laser was scanned over the whole range of the Doppler broadened Balmer-α line of atomic hydrogen. The wavelength scan spent 10 s. The relative frequency of the laser beam was monitored using a Fabry-Pérot spectrum analyzer. A small part of the laser beam was picked up using a beam sampler and was used as the probe beam. The probe beam was coupled to a polarization-maintained single-mode optical fiber with a core diameter of 3.5 μm. The other part of the laser beam was intensified using a diode laser amplifier (Toptica BoosTA), and was used as the pump beam. The pump beam was coupled to another polarization-maintained single-mode optical fiber. The optical fibers guided the laser beams to the vacuum chamber. The output beams from the optical fibers were collimated using lenses, and were injected into the plasma from the counter directions. The diameters (FHWM) of the collimated probe and pump beams at the edge of the electrode were approximately 0.3 mm. Both the paths of the probe and pump beams were parallel to the electrode surface. The two beams were crossed with a small angle of approximately 10 mrad above the center of the electrode. The distance between the electrode surface and the laser beams was variable. The polarizations of the laser beams were parallel to the sheath electric field. The powers of the probe and pump beams were 0.34 and 18.6 mW, respectively. The probe beam passed through the plasma was introduced into a photodiode detector via an interference filter at the Balmer-α line. The electrical signal from the photodiode was connected to a lock-in amplifier to observe the synchronous component with the modulation frequency of the rf power.

The Balmer-α line of atomic hydrogen was optically thin in the plasma used in the present experiment, and the magnitude of absorption was approximately 1×10^{-3}. In spite of the weak absorption, we succeeded in measuring the Doppler-broadened absorption spectrum of the probe beam clearly by modulating the rf power and by using the lock-in amplifier. When we introduced the pump beam from the counter direction to the probe beam, we observed several dips with narrow linewidths in the absorption spectrum. The dips were caused by

the saturation effect of fine-structure absorption lines. The maximum depth in the dips was approximately 20%. The saturation spectrum was obtained by calculating the difference between the absorption spectra with and without the pump beam. Figure 2 shows the saturation spectra which were observed at various distances between the laser beams and the electrode surface.

Figure 3 shows theoretical Stark spectra in the π polarization configuration (the polarizations of the laser beams are parallel to the sheath electric field), which were calculated using a perturbation theory by assuming various electric fields. The same homogeneous broadening width of 420 MHz, which was the widths of the peaks shown in Fig. 2(a), was assumed in Fig. 3 for all transition lines. The five peaks (labeled A-E) in the theoretical spectrum with no electric field (Fig. 3(a)) show fine structure components of the Balmer-α line. The detailed assignments are shown in Table I. The amplitudes of the $2p^2P^o_{1/2} - 3s^2S_{1/2}$ and $2p^2P^o_{3/2} - 3s^2S_{1/2}$ transitions are much smaller, and they are not seen in Fig. 3. The origin of the horizontal axis of Fig. 3 is the frequency of the $2p^2P^o_{3/2} - 3d^2D_{5/2}$ (peak B) transition. As shown in Fig. 3, in the theoretical spectra, the peak frequencies of the $2p^2P^o_{3/2} - 3d^2D_{5/2}$ (peak B) and $2p^2P^o_{1/2} - 3d^2D_{3/2}$ (peak E) transitions shifted toward the high-frequency side with the increase in the electric field strength. On the other hand, the frequencies of the $2p^2P^o_{3/2} - 3d^2D_{3/2}$ (peak A) and $2s^2S_{1/2} - 3p^2P^o_{1/2}$ (peak C) transitions shifted toward the low-frequency side. In addition, the linewidths of peaks A ($2p^2P^o_{3/2} - 3d^2D_{3/2}$) and D ($2s^2S_{1/2} - 3p^2P^o_{3/2}$) were broadened by Stark splitting, when the electric field is higher than 150 V/cm.

The five fine structure components listed in Table I are observed in the experimental saturation spectrum at a distance of 1.1 mm from the electrode, as shown in Fig. 2(a). The two peaks with label X in Fig. 2(a) are not found in the theoretical spectrum, but they are understood as cross-over peaks. The frequencies of the $2p^2P^o_{3/2} - 3d^2D_{3/2}$ (peak A) and $2p^2P^o_{3/2} - 3d^2D_{5/2}$ (peak B) transitions shifted toward the low- and high-frequency sides, respectively, when we moved the observation position toward the vicinity to the electrode surface. This is a consistent result with the theoretical Stark spectrum shown in Fig. 3. The frequency shifts of the $2s^2S_{1/2} - 3p^2P^o_{1/2}$ (peak C) and $2p^2P^o_{1/2} - 3d^2D_{3/2}$ (peak E) transitions were not observed in the experimental spectra shown in Fig. 2, suggesting that the electric field at a distance of 0.2 mm from the electrode surface is less than 150 V/cm. We observed the broadening of the $2p^2P^o_{3/2} - 3d^2D_{5/2}$ (peak B) and $2p^2P^o_{1/2} - 3d^2D_{3/2}$ (peak E) transition lines at a distance of 0.2 mm. However, the broadening of the two transition lines were negligible in the theoretical Stark spectra in electric fields less than 200 V/cm. The reason for

this discrepancy has not been understood yet, but a possibility is the contribution of the σ polarization component (the polarizations of the laser beams are perpendicular to the sheath electric field) in the experimental Stark spectra. Although we cannot show the data in the present paper, the theoretical calculation of the Stark effect in the σ polarization configuration shows the broadening of the $2p^2P^o_{3/2} - 3d^2D_{5/2}$ (peak B) line at an electric field of 150 V/cm.

According to the comparison between the experimental and theoretical Stark spectra shown in Figs. 2 and 3, it is considered that the frequency distance between peaks A ($2p^2P^o_{3/2} - 3d^2D_{3/2}$) and B ($2p^2P^o_{3/2} - 3d^2D_{5/2}$) can work as a measure for determining the electric field strength. The frequency distance between peaks A and B, which was obtained from theoretical Stark spectra, is plotted in Fig. 4 as a function of the electric field strength. The frequency distance between peaks A and B, which was obtained from the experimental Stark spectra, is shown in Fig. 5 as a function of the distance between the electrode surface and the laser beams. The horizontal error bars indicated in Fig. 5 show the ambiguity in the measurement position due to the diameter of the laser beam. It is considered from the theory of saturation spectroscopy that the width of the measurement area is $1/\sqrt{2}$ of the diameter of the laser beams, if we assume the perfect overlapping between the pump and probe beams. The vertical error bars in Fig. 5 are negligibly small, since the ambiguity in determining the frequency distance between peaks A and B from the experimental Stark spectra was 10 MHz, as will be described below. By comparing Figs. 4 and 5, we evaluated the spatial distribution of the electric field strength in the sheath region successfully, as shown in Fig. 6. Although the frequency distances between peaks A and B shown in Fig. 5 result in electric fields less than 5 V/cm at 0.6 and 1.0 mm from the electrode, they are not plotted in Fig. 6 since the measurement ambiguity (or the error bar) exceeds the evaluated electric field strengths. The voltage that is evaluated by integrating the electric field distribution shown in Fig. 6 is approximately 5 V. This voltage is slightly lower than the plasma potential without placing the electrode, but the difference could be compensated partly by the voltage sustained in the presheath region.

Although the saturation spectrum shown in Fig. 2(a) has a linewidth of 420 MHz, we can identify much smaller shifts of the peak positions of the transition lines. The minimum change in the distance between peaks A and B, which we could identify experimentally, was 10 MHz. According to Fig. 4, the change of 10 MHz in the frequency distance between peaks A and B corresponds to the electric field of 10 V/cm. This is a more sensitive detection limit than those of conventional laser optogalvano spectroscopy and laser-induced collisional fluorescence spectroscopy, and is close to the detection limit of laser-induced fluorescence-

dip spectroscopy. In addition, a sensitivity higher than 10 V/cm is meaningless in practical plasma diagnostics, since it was observed that the static electric field was masked by microfields (Holtsmark fields) which was approximately 10 V/cm in typical low-temperature plasmas.[14,15] Therefore, the sensitivity of 10 V/cm is sufficient when we apply the developed method to the diagnostics of low-temperature plasmas.

A difficulty of the developed method is caused by the fact that the Balmer-α line of atomic hydrogen is optically thin in usual low-temperature plasmas. In this work, we amplified the absorption spectrum by modulating the plasma production, however, the pulse modulation of the plasma production is not applicable in many experimental conditions. An alternative method is modulating the pump laser beam using an optical chopper and operating the lock-in amplifier with the reference signal at the frequency of the optical modulation. We have succeeded in measuring Stark spectra which are similar to those shown in Fig. 2 in a cw hydrogen plasma by using this method, and the results will be reported in a separate paper.

In conclusion, we have succeeded in measuring the Stark spectra of the Balmer-α line of atomic hydrogen in the sheath region of a hydrogen plasma by applying saturation spectroscopy with a fine spectral resolution. The detection limit of the electric field is 10 V/cm, which is a sufficient sensitivity for investigating the structures of the sheath electric fields in low-temperature plasmas. The measurement system employs a tunable diode laser, hence it is more economical than the conventional system of laser Stark spectroscopy. In addition, since the diode laser system is easy to use, the developed system is useful in various experiments which need the measurements of electric fields in plasmas.

References

1) M. A. Lieberman and A. J. Lichtenberg, *Principles of Plasma Discharges and Materials Processing, 2nd ed.* (Wiley, New York, 2005).
2) J. W. Coburn and H. F. Winters, J. Vac. Sci. Technol. **16**, 391 (1979).
3) N. Hershkowitz, Phys. Plasmas **12**, 055502 (2005).
4) D. K. Doughty and J. E. Lawler, Appl. Phys. Lett. **45**, 611 (1984).
5) B. N. Ganguly, J. R. Shoemaker, B. L. Preppernau, and A. Garsccadden, J. Appl. Phys. **61**, 2778 (1987).
6) B. L. Preppernau and B. N. Ganguly, Rev. Sci. Instrum. **64**,1414 (1993).
7) V. P. Gavrilenko, H. J. Kim, T. Ikutake, J. B. Kim, T. W. Choi, M. D. Bowden, and K. Muraoka, Phys. Rev. E **62**, 7201 (2000).
8) K. E. Greenberg and G. A. Hebner, Appl. Phys. Lett. **63**, 3282 (1993).
9) M. D. Bowden, Y. W. Choi, K. Muraoka, and M. Maeda, Appl. Phys. Lett. **66**, 1059 (1995).
10) Y. W. Choi, M. D. Bowden, and K. Muraoka, Appl. Phys. Lett. **69**, 1361 (1996).
11) J. B. Kim, K. Kawamura, Y. W. Choi, M. D. Bowden, K. Muraoka, and V. Helbig, IEEE Trans. Plasma Sci. **26**, 1556 (1998).
12) U. Czarnetzki, D. Luggenhölscher, and H. F. Döbele, Phys. Rev. Lett. **81**, 4592 (1998).
13) T. Kampschulte, J. Schulze, D. LuggenhÏscher, M. D. Bowden, and U. Czarnetzki, New J. Phys. **9**, 18 (2007).
14) K. Takizawa, K. Sasaki, and K. Kono, Appl. Phys. Lett. **84**, 185 (2004).
15) K. Takizawa, A. Kono, and K. Sasaki, Appl. Phys. Lett. **90**, 011503 (2007).
16) K. Takizawa and K. Sasaki, Jpn. J. Appl. Phys. **46**, 6822 (2007).
17) E. V. Barnat and G. A. Hebner, Appl. Phys. Lett. **85**, 3393 (2004).
18) E. V. Barnat and G. A. Hebner, J. Appl. Phys. **96**, 4762 (2004).
19) E. Wagenaars, G. M. W. Kroesen, and M. D. Bowden, Phys. Rev. A **74**, 033409 (2006).
20) M. G. Adamov, A. Steiger, K. Grẗzmacher, and J. Seidel, Phys. Rev. A **75**, 013409 (2007).
21) R. Asakawa, M. Goto, N. Sadeghi, and K. Sasaki, J. Instrum. **7**, C01018 (2012).

Table I. Assignments of the fine-structure components shown in Figs. 2 and 3.

Label	Lower state	Upper state	Wavelength (nm)
A	$2p^2P^o_{3/2}$	$3d^2D_{3/2}$	656.2867
B	$2p^2P^o_{3/2}$	$3d^2D_{5/2}$	656.2852
C	$2s^2S_{1/2}$	$3p^2P^o_{1/2}$	656.2772
D	$2s^2S_{1/2}$	$3p^2P^o_{3/2}$	656.2725
E	$2p^2P^o_{1/2}$	$3d^2D_{3/2}$	656.2710

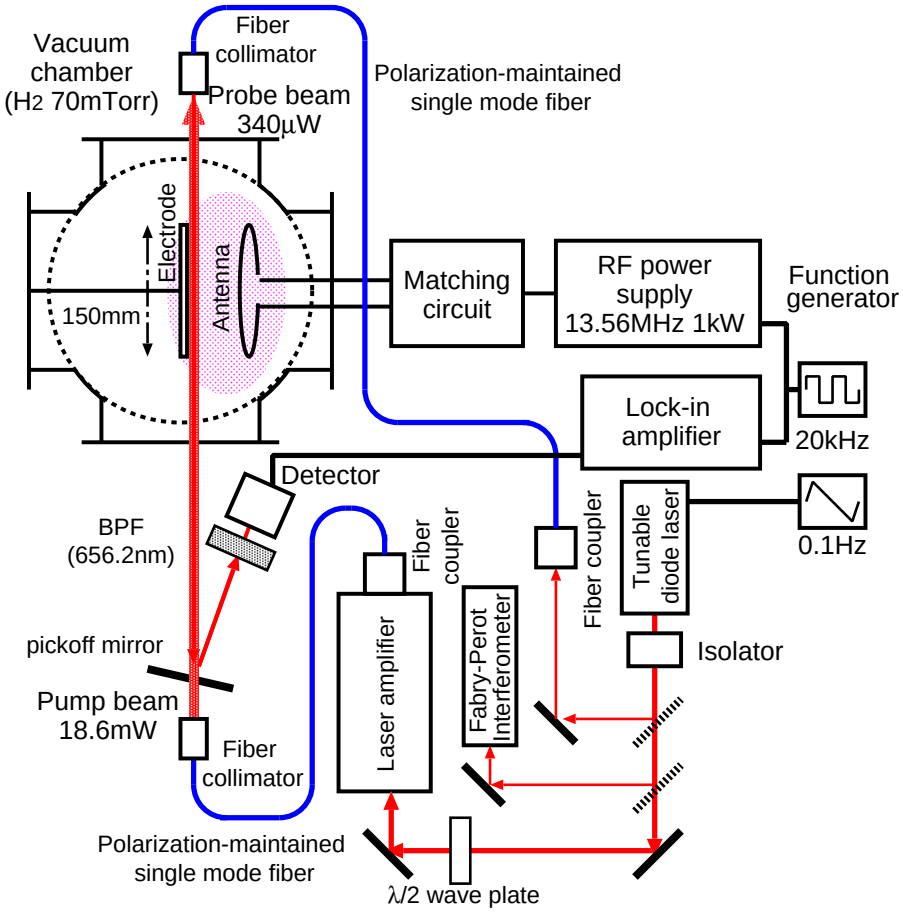

Fig. 1. Schematic of experimental apparatus.

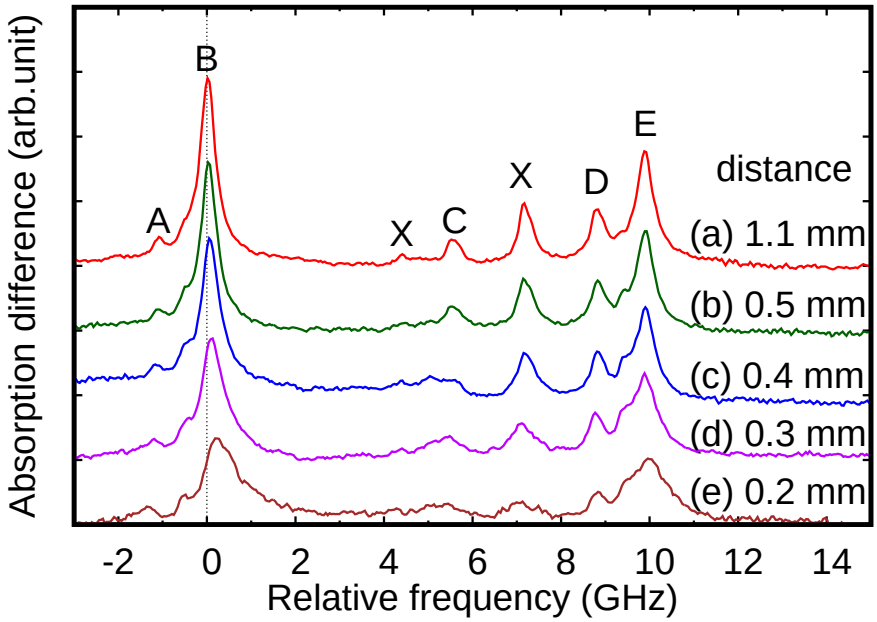

Fig. 2. Saturation spectra observed at various distances from the electrode surface. The polarizations of the pump and probe beams were parallel to the sheath electric field (π polarization configuration). The assignments of the peaks A-E are shown in Table I. The peaks with label X are understood as the cross-over components.

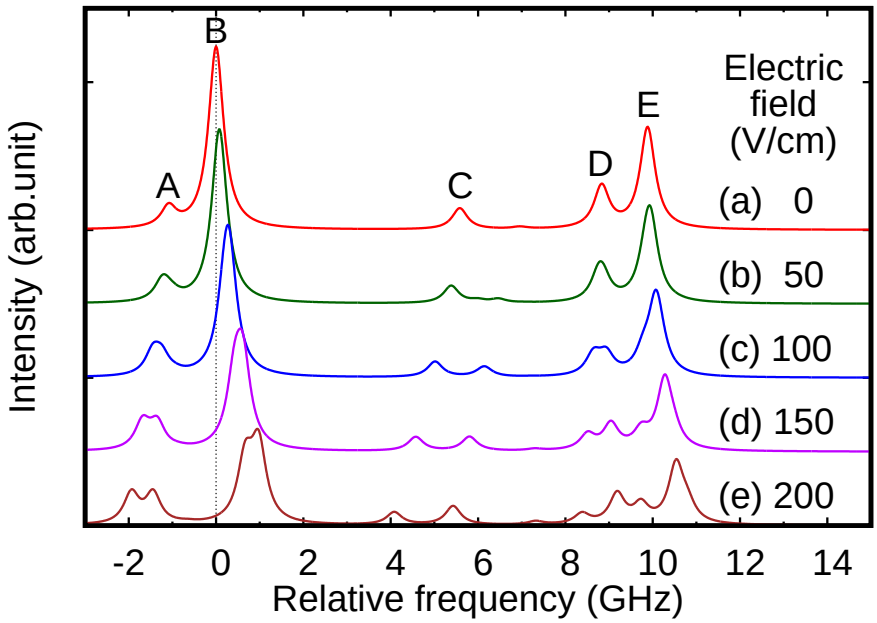

Fig. 3. Theoretical saturation spectra of the Balmer-α line of atomic hydrogen in π polarization configuration. Various electric fields between 0 and 200 V/cm are assumed. The assignments of the peaks A-E are shown in Table I.

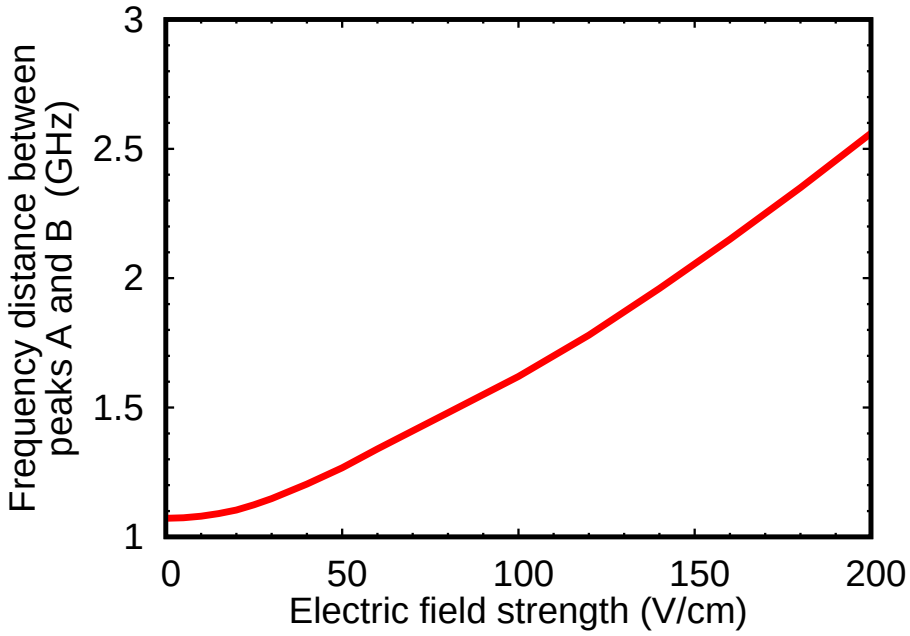

Fig. 4. Frequency distance between peaks A and B in the theoretical Stark spectra as a function of the electric field strength.

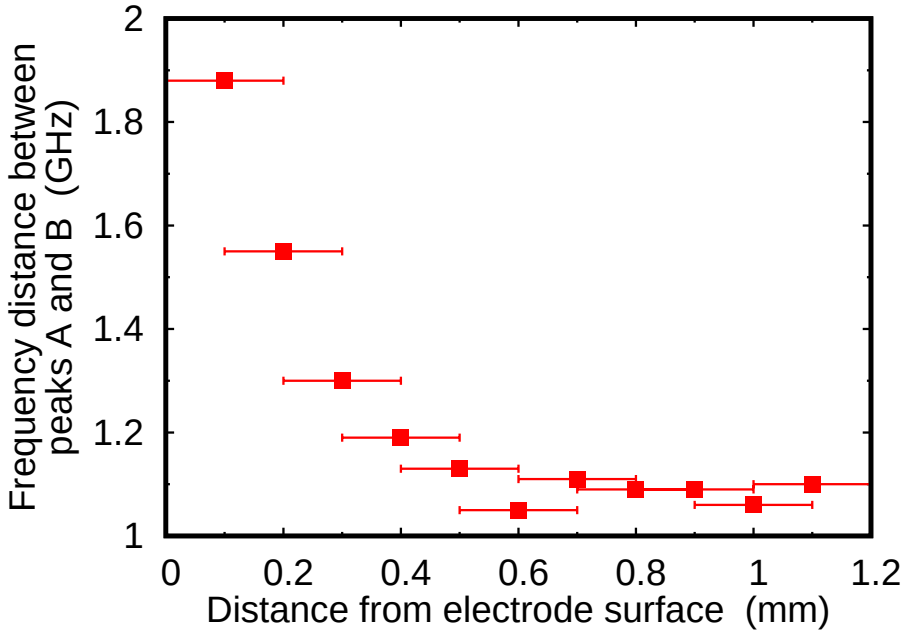

Fig. 5. Frequency distance between peaks A and B in the experimental Stark spectra as a function of the distance from the electrode surface.

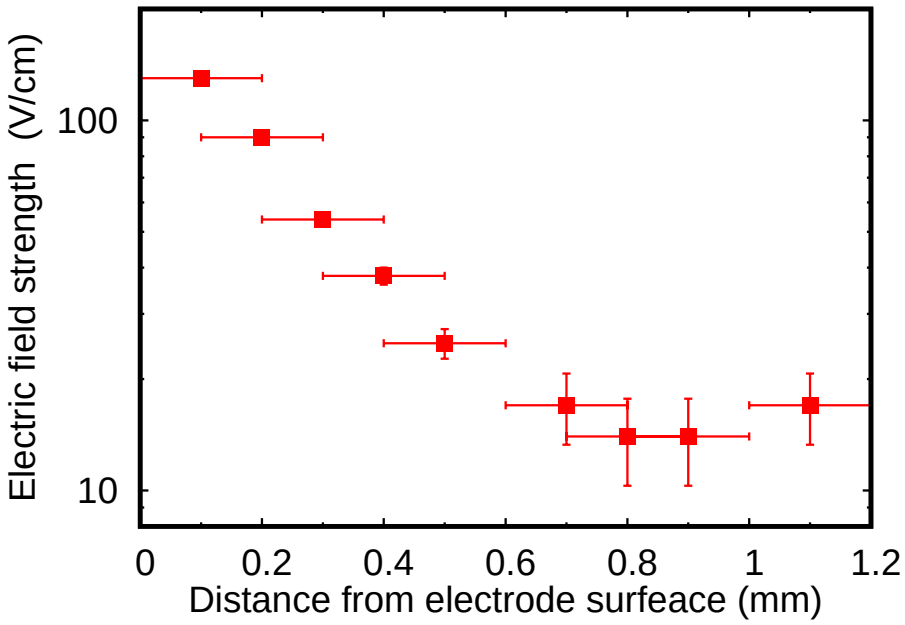

Fig. 6. Spatial distribution of the sheath electric field. The electric field was evaluated by comparing Figs. 4 and 5.